

Room-temperature bistability in a cobalt-octacyanidotungstate framework showing a charge-transfer phase transition with a red-blue color change

Kazuki Nakamura,^a Koji Nakabayashi,^{a*} Kenta Imoto,^a and Shin-ichi Ohkoshi,^{a*}

^a Department of Chemistry, School of Science, The University of Tokyo
7-3-1 Hongo, Bunkyo-ku, Tokyo 113-0033, Japan.

*To whom correspondence should be addressed
E-mail: ohkoshi@chem.s.u-tokyo.ac.jp

	Contents	Page
1	SEM-EDX images of CsHCoW (Figure S1)	S2
2	Thermogravimetric analysis of CsHCoW (Figure S2)	S3
3	IR spectrum of CsHCoW (Figure S3)	S4
4	Crystallographic data from Rietveld analysis of the HT phase of CsHCoW (Table S1)	S5
5	Crystal structure of the HT phase of CsHCoW (Figure S4)	S6
6	Hydrogen bonds and close contacts around H_5O_2^+ and Cs^+ ions in the HT phase of CsHCoW (Figure S5)	S7
7	Crystallographic data from Rietveld analysis of the LT phase of CsHCoW (Table S2)	S8
8	Crystal structure of the LT phase of CsHCoW (Figure S6)	S9
9	Hydrogen bonds and close contacts around H_5O_2^+ and Cs^+ ions in the LT phase of CsHCoW (Figure S7)	S10
10	Bond lengths between Co-N atoms from the Rietveld analyses for the PXRD patterns of each phase of CsHCoW (Table S3)	S11
11	Variable-temperature PXRD patterns of CsHCoW (Figure S8)	S12
12	UV-vis spectra of HT and LT phases of CsHCoW at room temperature (Figure S9)	S13
13	Thermodynamic quantities obtained from the DSC (Figure S10, Table S4)	S14

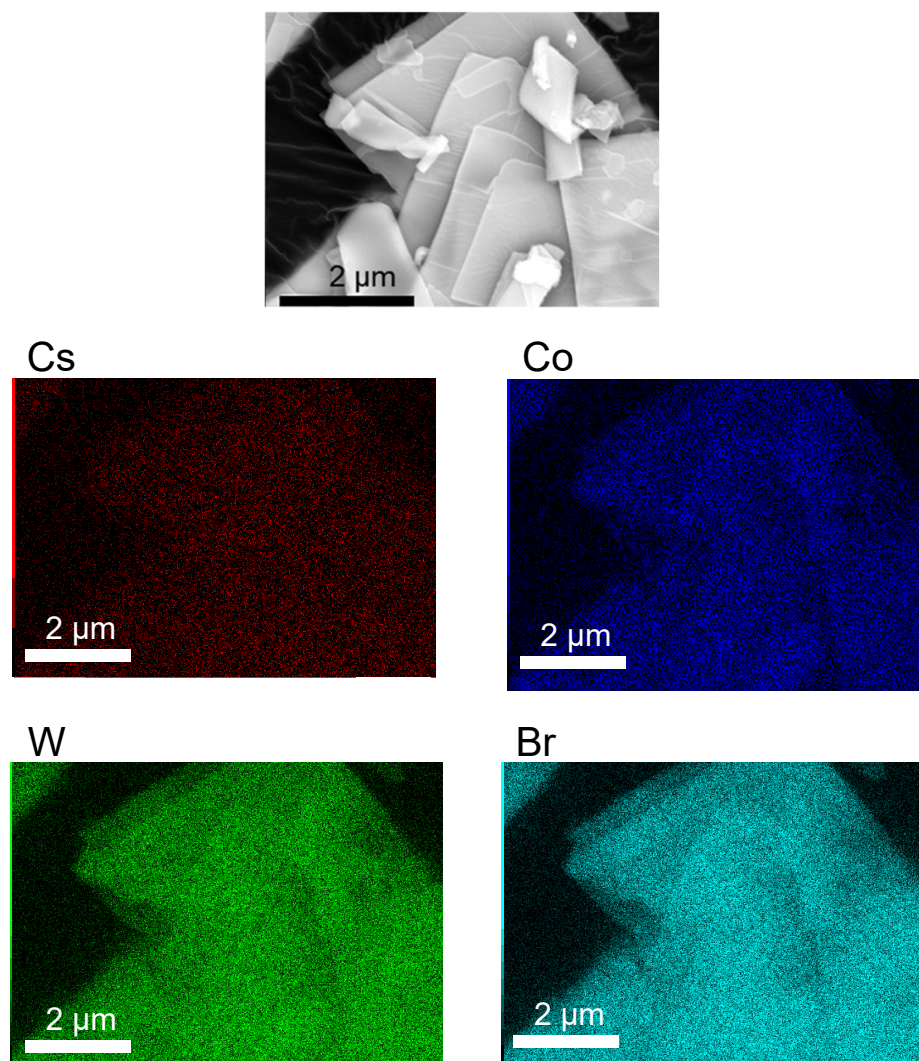


Figure S1. SEM image of **CsHCoW** (top) and SEM-EDX images with elemental mapping of Cs, Co, W, and Br (middle, bottom).

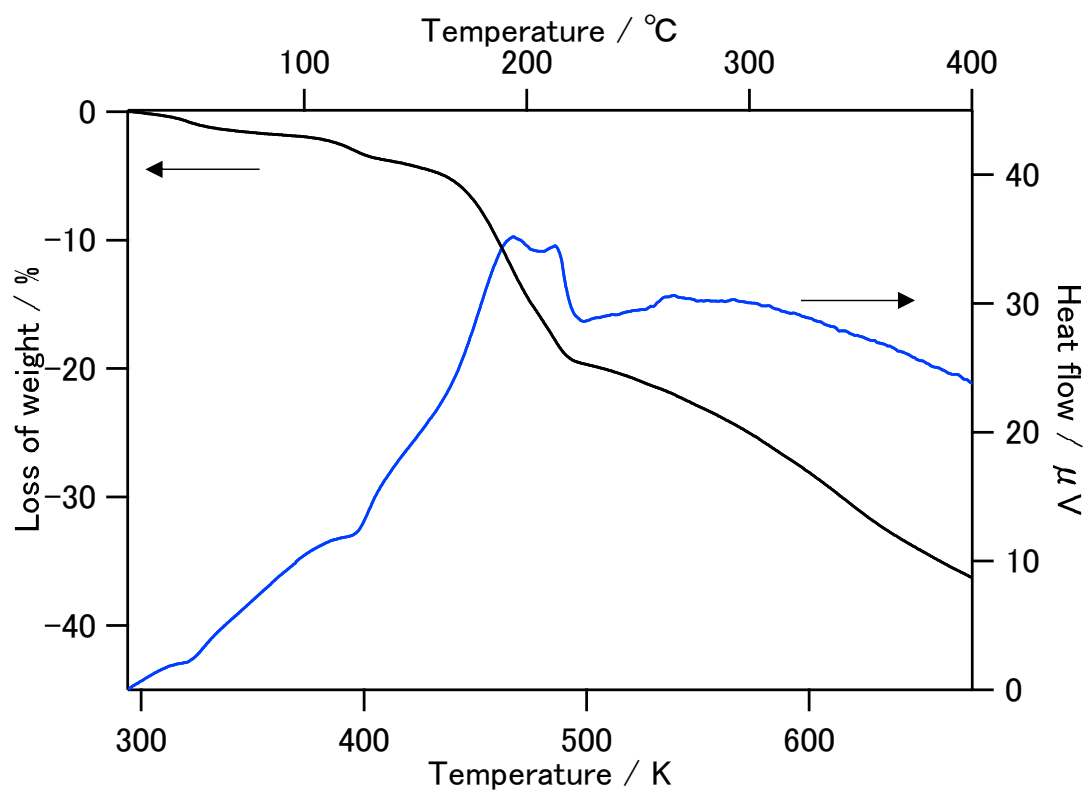


Figure S2. TG-DTA analysis under a scan rate of 5 K min^{-1} . The black and blue lines indicate the loss of weight and the heat flow, respectively.

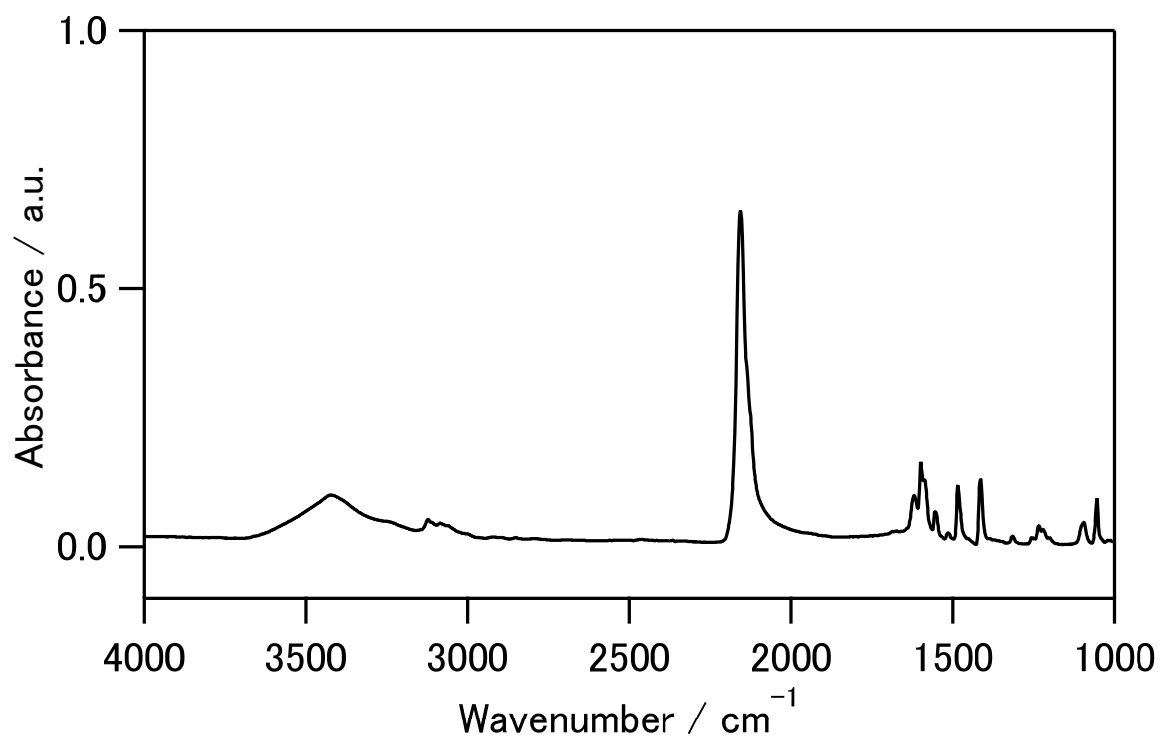


Figure S3. IR spectrum of CsHCoW in a KBr pellet at room temperature.

Table S1. Crystallographic data from Rietveld analysis for the PXRD pattern of the HT phase of **CsHCoW**.

Crystal system	Monoclinic
Space group	$P2_1/c$
$a / \text{\AA}$	13.2626(8)
$b / \text{\AA}$	14.1740(12)
$c / \text{\AA}$	15.3609(8)
$\beta / ^\circ$	106.596(6)
Z	4
$V / \text{\AA}^3$	2767.3(3)
$R_{\text{wp}} / R_{\text{p}}$	0.0420 / 0.0311
S	2.6607
T / K	293

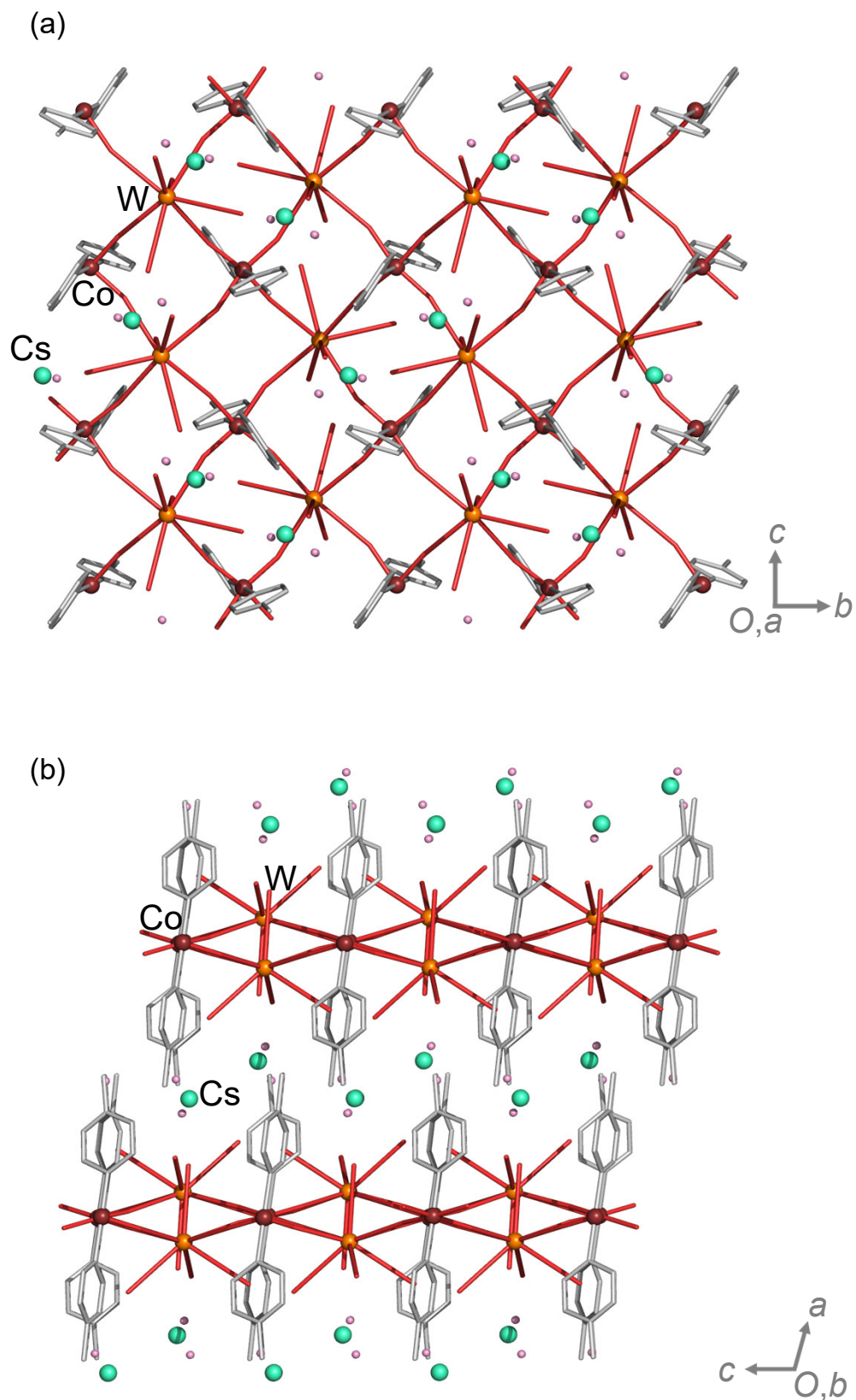


Figure S4. Crystal structure of the HT phase of CsHCoW . The light green, red, orange, and pink spheres indicate Cs, Co, W, and O respectively. (a) View from the a axis. (b) View from the b axis.

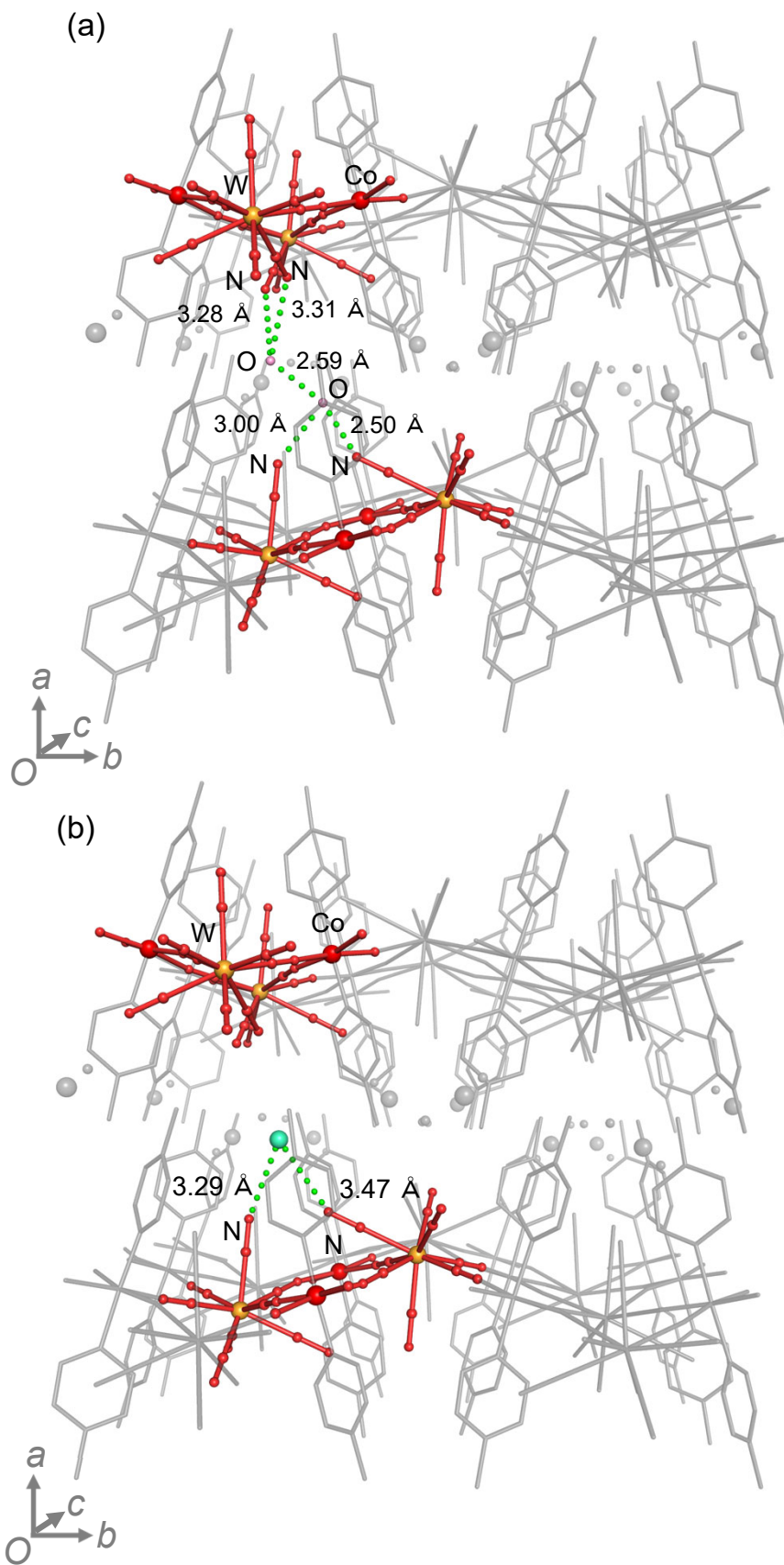


Figure S5. Hydrogen bonds between a H_5O_2^+ ion and cyanido groups of $[\text{W}(\text{CN})_8]^{3-}$ (a) and close contacts between a Cs^+ ion and cyanido groups of $[\text{W}(\text{CN})_8]^{3-}$ (b) in the HT phase of CsHCoW .

Table S2. Crystallographic data from Rietveld analysis for the PXRD pattern of LT phase of **CsHCoW**. The powder sample of the LT phase was prepared by cooling of the HT phase with liquid N₂. After the cooling, the LT phase was sustained even at room temperature due to the existence of the thermal hysteresis over room temperature. The PXRD measurement was conducted at 293 K.

Crystal system	Monoclinic
Space group	$P2_1/c$
$a / \text{\AA}$	13.1330(7)
$b / \text{\AA}$	13.7128(9)
$c / \text{\AA}$	14.6941(14)
$\beta / ^\circ$	106.116(7)
Z	4
$V / \text{\AA}^3$	2542.3(3)
$R_{\text{wp}} / R_{\text{p}}$	0.0417 / 0.0298
S	2.7592
T / K	293

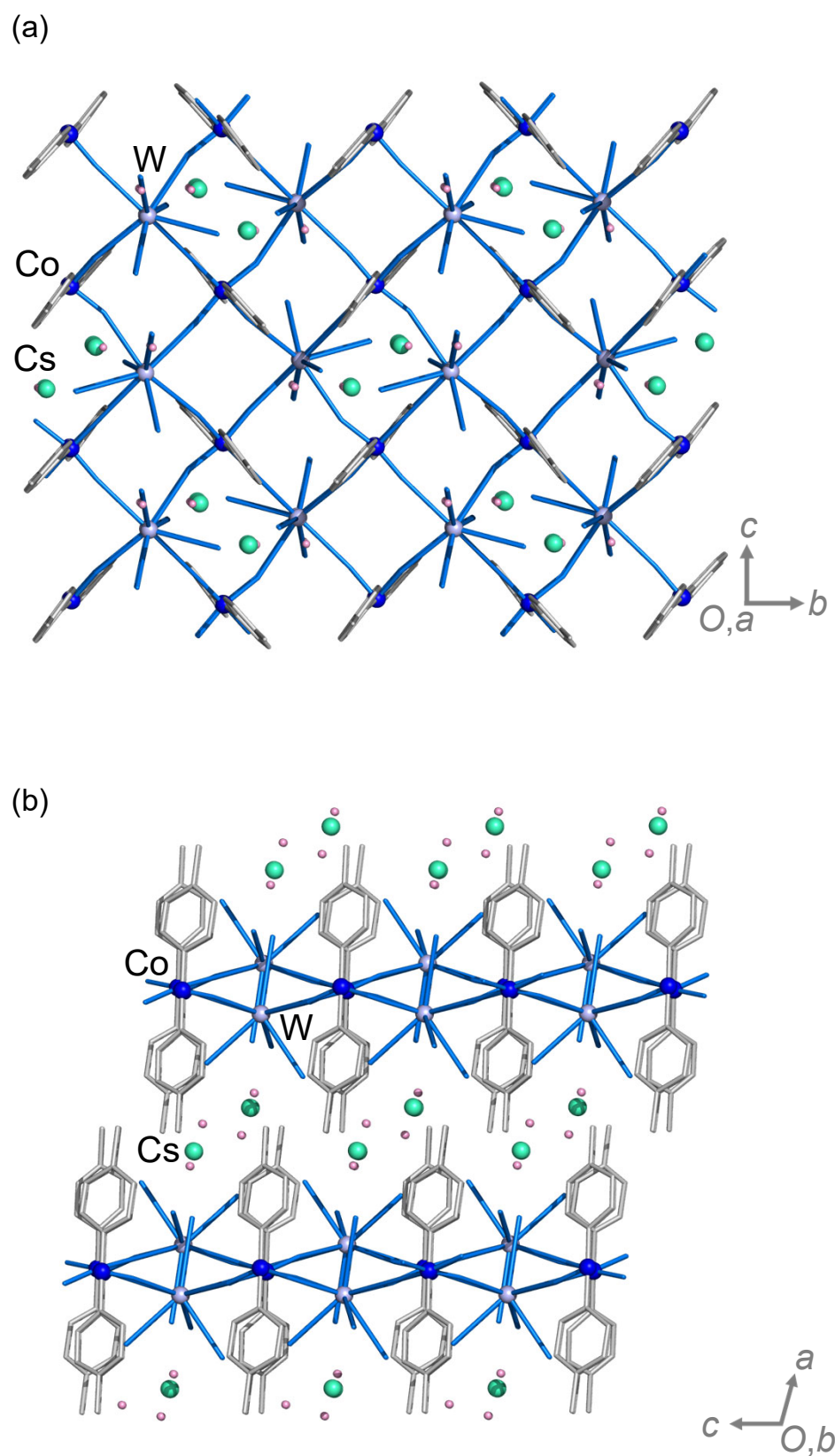


Figure S6. Crystal structure of the LT phase of CsHCoW . The light green, blue, light blue, and pink spheres indicate Cs, Co, W, and O respectively. (a) View from the a axis. (b) View from the b axis.

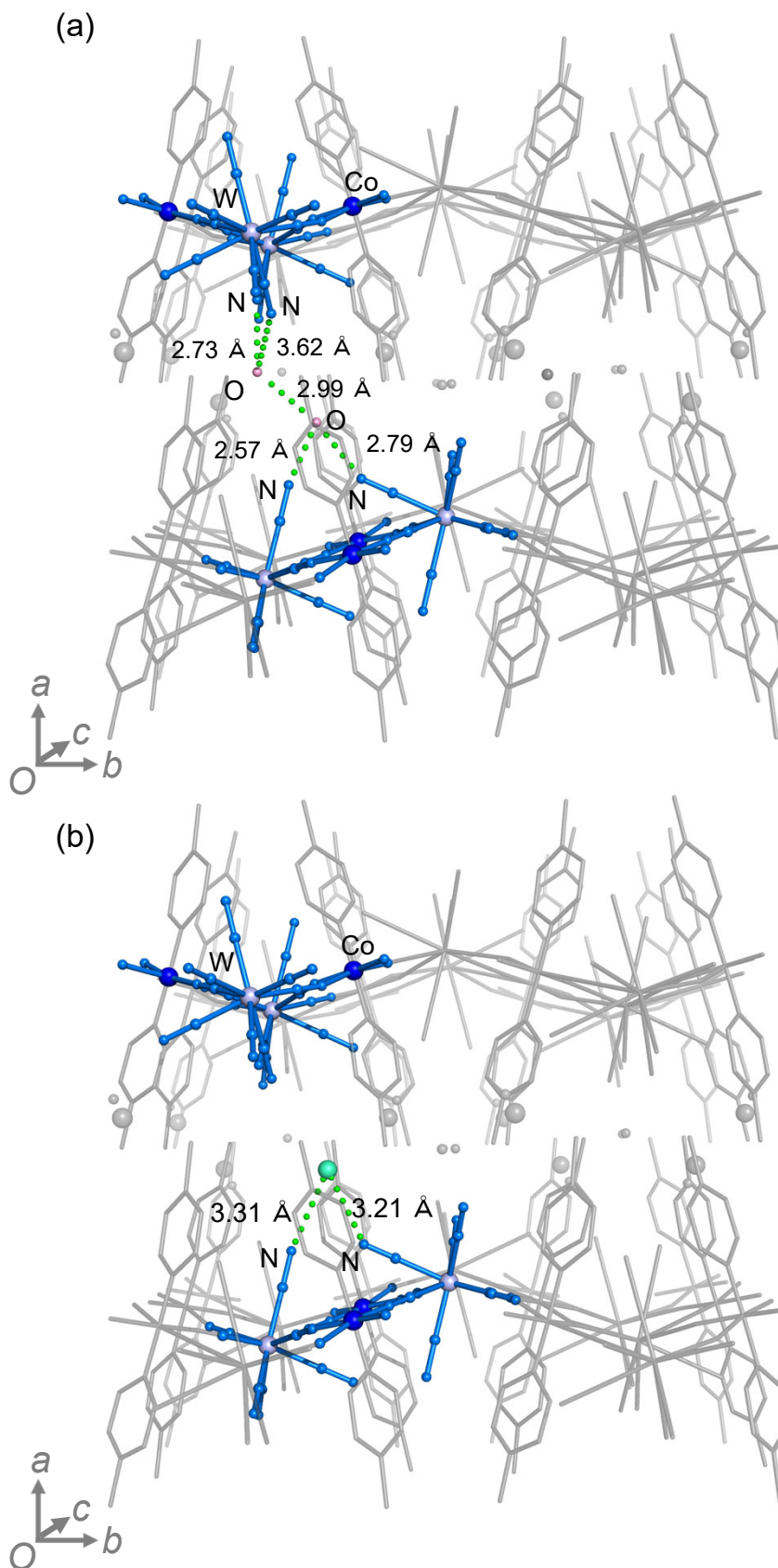


Figure S7. Hydrogen bonds between a H_5O_2^+ ion and cyanido groups of $[\text{W}(\text{CN})_8]^{3-}$ (a) and close contacts between a Cs^+ ion and cyanido groups of $[\text{W}(\text{CN})_8]^{3-}$ (b) in the LT phase of CsHCoW .

Table S3. Bond lengths (Å) between Co-N atoms for the HT and LT phases of CsHCoW.

	Bond	HT phase	LT phase
equatorial	Co1-N1	2.124	1.886
	Co1-N2	2.096	1.954
	Co1-N3	2.214	1.936
	Co1-N4	2.118	1.828
axial	Co1-N9	2.178	1.853
	Co1-N10	2.166	1.855
Average of Co1-N bond length		2.149	1.885

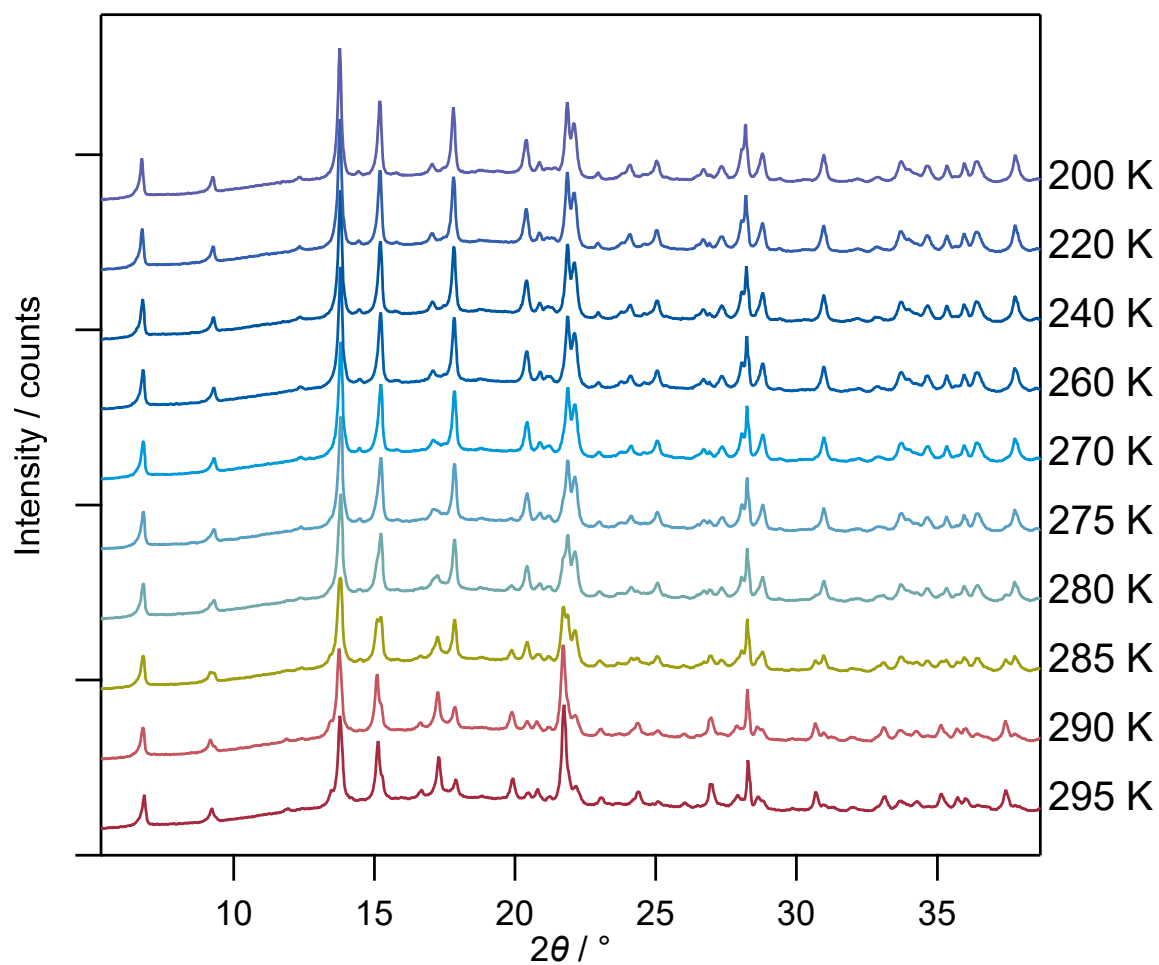


Figure S8. Variable temperature PXRD patterns of **CsHCoW** at respective temperatures under the cooling process. The sharpe peak at 28° represents the diffraction from the Si standard.

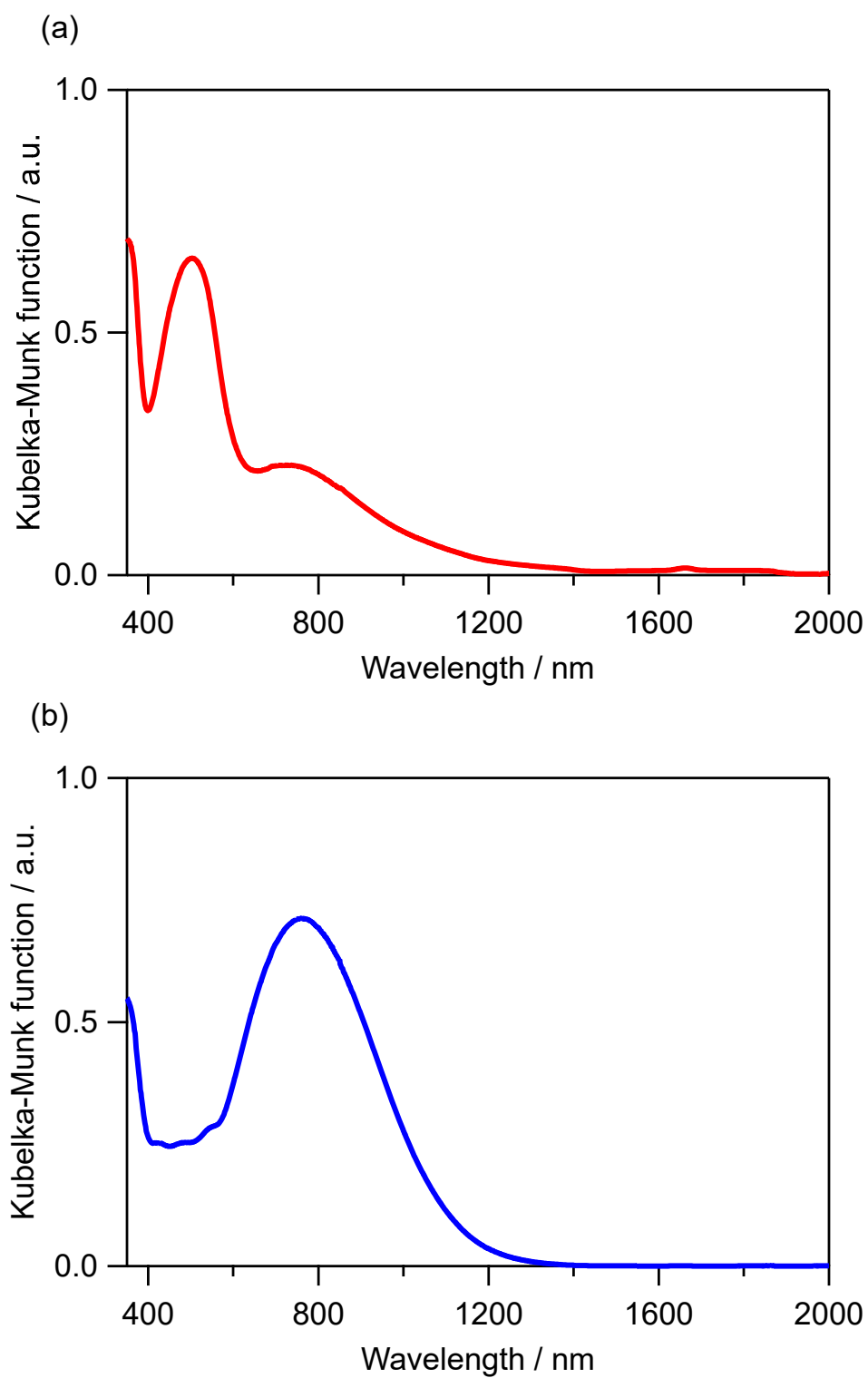


Figure S9. UV-vis spectra of HT (top) and LT (bottom) phases of **CsHCoW** in the range of 350-2000 nm at room temperature.

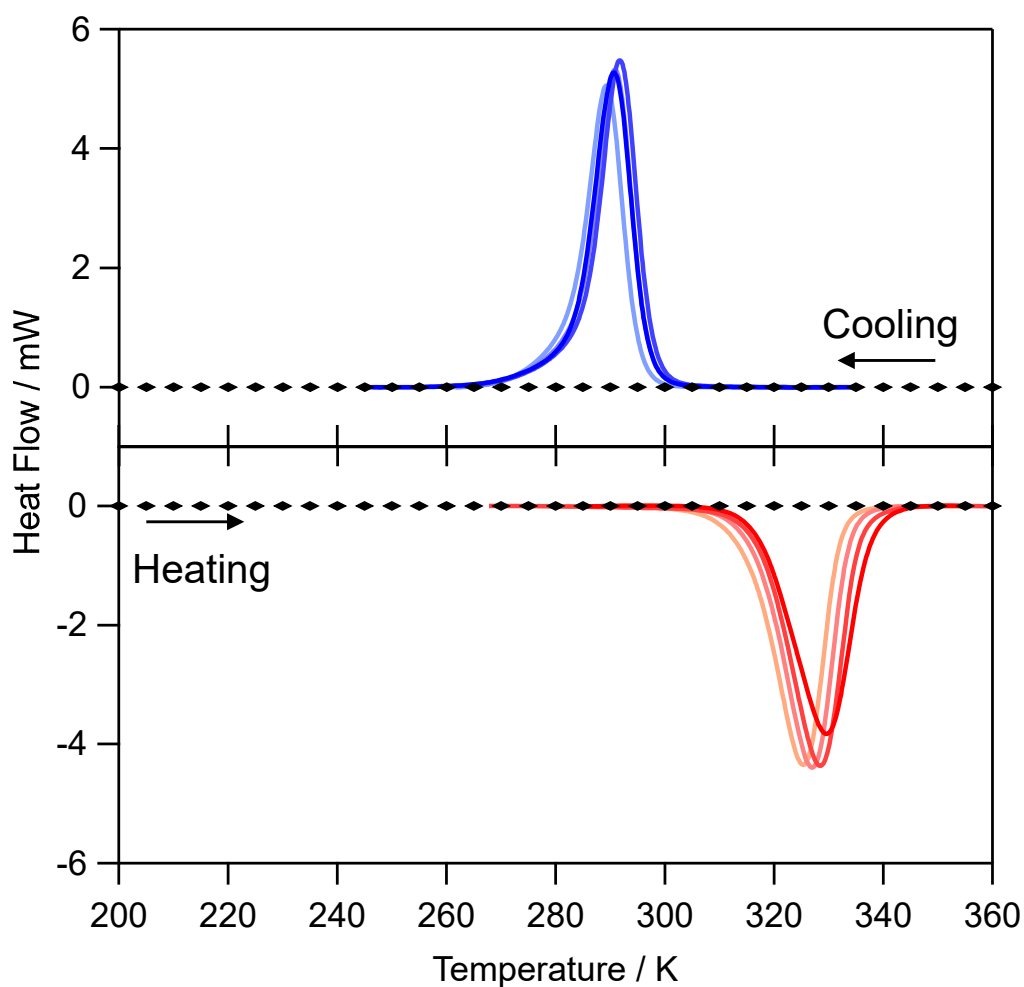


Figure S10. The 1st to 4th cycles in the DSC measurement for **CsHCoW** in the range of 200-360 K recorded under a temperature sweeping rate of 10 K min⁻¹. Blue and red lines indicate the cooling and heating processes, respectively.

Table S4. Transition temperature, enthalpy, and entropy of the phase transition in each cooling-heating cycle in Figure S10.

Cycle No	Cooling			Heating		
	T / K	$\Delta H / \text{kJ mol}^{-1}$	$\Delta S / \text{J K}^{-1} \text{mol}^{-1}$	T / K	$\Delta H / \text{kJ mol}^{-1}$	$\Delta S / \text{J K}^{-1} \text{mol}^{-1}$
1	291	-25.9	89.1	330	26.5	80.4
2	292	-26.5	90.1	329	26.5	80.8
3	291	-25.8	88.6	327	25.3	77.3
4	289	-24.7	85.4	326	25.3	77.8